A Combinatorial Impairment-Compensation Digital Predistorter for a Sub-GHz IEEE 802.11af-WLAN CMOS Transmitter Covering a 10x-Wide RF Bandwidth

Chak-Fong Cheang, *Student Member, IEEE*, Ka-Fai Un, *Student Member, IEEE*, Wei-Han Yu, *Student Member, IEEE*, Pui-In Mak, *Senior Member, IEEE*, and Rui P. Martins, *Fellow, IEEE*

***Abstract*—A new combinatorial impairment-compensation digital predistorter (DPD) for a sub-GHz IEEE 802.11af-WLAN CMOS transmitter (TX) is proposed. For the TX to cover a 10x-wide bandwidth, the DPD implements a modified dynamic deviation reduction (DDR)-based Volterra series to jointly nullify the frequency-dependent I/Q imbalance, counter-intermodulation (CIM) of mixers, and nonlinearities of power amplifier (PA) with memory effect. The interactions of those impairments are firstly analyzed using two Volterra series. After applying the tandem properties of Volterra series, interactions of all impairments can be described in one Volterra series by bonding those impairments in parallel. Coefficients of the DPD are extracted with the Least- Square (LS) estimator, achieving lower running complexity than the existing DPDs, which were developed to handle the PA nonlinearities only. Verifications are based on both system-level simulations and silicon measurements of a 65-nm CMOS TX prototype. When the TX delivers a 6-MHz bandwidth, 2048-point, 64-QAM OFDM signal at $> +10$ dBm output power, the measured EVM is $<3.7\%$ and adjacent channel leakage ratio (ACLR) is < -40.2 dBc under individual DPD applied at each RF. A novel one-shot calibration for reuse in the entire TV-band is demonstrated also, showing EVM $<4.2\%$ and ACLR < -39.8 dBc.**

***Index Terms*—CMOS, counter-intermodulation (CIM), digital predistortion (DPD), frequency-dependent I/Q imbalance, power amplifier (PA), RF, Volterra series, wideband transmitter.**

I. Introduction

THE IEEE 802.11af-WLAN standard [1] is opening up a new perspective for flexible utilization of the unoccupied TV spectrum. Sub-GHz communications are not only capable of propagation to a longer distance when compared with the 2.4 and 5-GHz WLANs due to lower path loss, but also show better penetration of obstacles (e.g., wall). Cognitive-radio transmitter (TX), which includes a wideband modulator (MOD) and a power amplifier (PA), is one of the key enablers for TV white space (TVWS) transmission. Yet a sub-GHz TX [2], [3] will have a strong bandwidth-dependent [4] memory effect accompanied with the PA nonlinearities at low frequency (e.g., when a 6-MHz bandwidth signal is transmitted at a 54-MHz RF). Also, amplitude- and frequency-dependent [4] memory effect can be induced by the impedance of the matching network. These nonidealities penalize the error vector magnitude (EVM) and induce an asymmetrical spectral regrowth to the adjacent channels, hindering the performance of orthogonal frequency-division multiplexing (OFDM) signals. Besides the nonlinearities with memory effect of the PA, the frequency-dependent I/Q imbalance [5], [6] and the counter-intermodulations (CIMs) [7], [8] of the MOD also affect the EVM and adjacent channel leakage ratio (ACLR). To compensate those impairments, digital techniques are attractive and have been widely studied in [6], [7] and [9]–[12]. Yet most impairment is handled separately, and calls for add-on RF switches [10] or a second feedback loop [5]. Any compensation techniques for frequency-dependent I/Q imbalance can be affected by the digital predistortion (DPD) if it resolves just the memory effect of the PA. As a result, a combinatorial DPD jointly addressing more impairment will be attractive. In the prior art, the LOFT and image components are compensated together with the PA nonlinearities with realistic complexity. Yet the employed look-up table [11] and memory polynomial [12] are only suitable for memoryless or low memory effect systems. Volterra-series based DPD is common to address the PA nonlinearities with moderate/strong memory effect [9], [13]–[15]. Yet the EVM and ACLR achieved by the DPD can become worse if the impairments of TX are not handled properly. To our knowledge, only [6] applies the Volterra-series to address the I/Q imbalance, but it is restricted to weakly-nonlinear systems and has higher complexity.

This work aims at an effective DPD that can jointly mitigate the frequency-dependent I/Q imbalance and PA nonlinearities. The interaction between CIMs and the nonlinearities [7] are also compensated. As the computational complexity grows up exponentially to describe all the impairments via a Volterra-series predistorter, a modified dynamic-derivation-reduction-based (DDR) Volterra series predistorter is proposed to reduce the complexity. Measurements of a 54-to-600-MHz TX in 65-nm CMOS validate that the proposed predistorter achieves

Manuscript received September 15, 2014; revised November 15, 2014; accepted January 06, 2015. Date of current version March 27, 2015. This work was supported by the University of Macau (MYRG114-FST13-MPI) and Macao Science and Technology Development Fund (FDCT)—SKL Fund. This paper was recommended by Associate Editor R. Gomez-Garcia.

C.-F. Cheang, K.-F. Un, W.-H. Yu and P.-I. Mak are with the State-Key Laboratory of Analog and Mixed-Signal VLSI and Faculty of Science and Technology, Department of ECE, University of Macau, Macao, China (e-mail: pimak@umac.mo).

R. P. Martins is with the State-Key Laboratory of Analog and Mixed-Signal VLSI and Faculty of Science and Technology, Department of ECE, University of Macau, Macao, China, and also with Instituto Superior Técnico, Universidade de Lisboa, 1049-001 Lisboa, Portugal (e-mail: rmartins@umac.mo).

Color versions of one or more of the figures in this paper are available online at http://ieeexplore.ieee.org.

Digital Object Identifier 10.1109/TCSI.2015.2390561

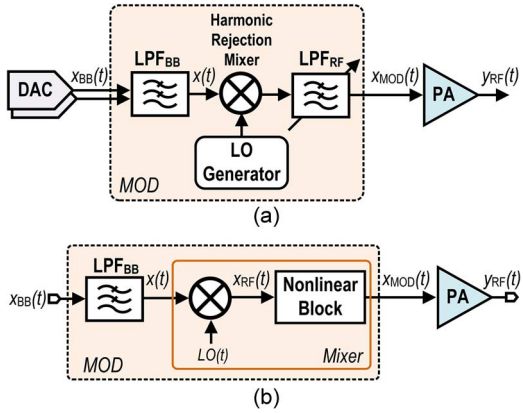

Fig. 1. (a) Block diagram of the transmitter and (b) its equivalent model.

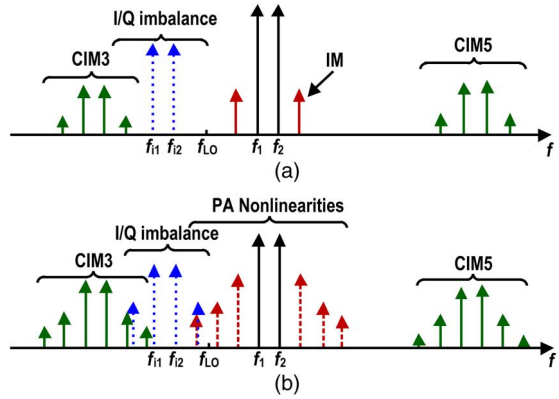

Fig. 2. The close-in spectrum of (a) MOD and (b) PA under the two-tone test.

an ACLR < -43 dBc and an EVM $<4.2\%$ over the whole TV band, conforming to the IEEE 802.11af WLAN specifications. The running complexity is also relaxed when comparing with the DPD of [15] $(r = 2)$. Finally, for the first time, one-shot mitigation of TX impairments for reuse in the entire TV-band is investigated, which reduces the number of compensation and computational power while keeping a satisfactory performance.

This paper is organized as follows: the nonlinear distortion analysis via Volterra series is introduced in Section II. The proposed predistorter and its running complexity are detailed in Section III. The experimental results are given in Section IV, and the paper is concluded in Section V.

II. Nonlinear Distortion Analysis Via Volterra Series

The simplified schematic of our wideband TX is depicted in Fig. 1(a). The I/Q baseband (BB) signals provided by the digital-to-analog converters are lowpass-filtered first. The BB signals are then up-converted to RF by the harmonic-rejection mixer. The RF signal is further purified by a tunable harmonic-rejection filter to suppress the harmonic products of the mixer under hard switching. Finally, the output signal of the MOD $x_{\mathrm{MOD}}(t)$ is delivered via a wideband PA. Based on this system model, the impairments of the MOD and PA are analyzed.

A. Impairments of MOD

Fig. 2(a) depicts the close-in spectrum of a MOD under a two-tone input. The impairments include the inter-modulations (IMs), and the CIMs due to mixer nonlinearity, and the image due to I/Q imbalance. Firstly, the nonlinearity of the mixer is considered. The harmonic-rejection mixer and filter can be modeled as a quadrature mixer with the local oscillator (LO) considered as a harmonic-rejected signal $LO(t)$ followed by a nonlinear block [Fig. 1(b)]. $LO(t)$ can be expressed as

$$LO(t) = \sum_{n=-\infty}^{\infty} g_n e^{j2n\pi f_{LO}t} \tag{1}$$

where g_{n} is the Fourier coefficient of the LO with n-odd harmonic and f_{LO} is the LO frequency. Thus, $x_{\mathrm{RF}}(t)$ can be expressed as [7],

$$x_{\mathrm{RF}}(t) = \sum_{n=odd} g_n \left(\mathrm{Re}\left[x(t)\right] + \mathrm{Im}\left[x(t)\right] e^{jn\frac{\pi}{2}}\right) e^{j2n\pi f_{LO}t} \tag{2}$$

With the presence of mixer nonlinearity, the output of the MOD can be written as

$$x_{\mathrm{MOD}}(t) = x_{\mathrm{RF}}(t) + a_3 x_{\mathrm{RF}}^3(t) + a_5 x_{\mathrm{RF}}^5(t) + \cdots \tag{3}$$

where a_n are the coefficients of the nth-order nonlinearity. The even-order terms can be ignored due to the differential circuitry. Substituting (2) into (3), $x_{\mathrm{MOD}}(t)$ can be derived as

$$\begin{aligned} x_{\mathrm{MOD}}(t) &= \{x(t) + 3a_3 \\ &\quad \times \left[\left(1 + 2|b_3|^2 + 2|b_5|^2 + 2b_3^* b_5\right)|x(t)|^2 x(t) \right. \\ &\quad \left. + \left(b_3 + b_3^2 b_5^*\right)\left(x^*(t)\right)^3\right]\} e^{j2\pi f_{LO}t} + \cdots \end{aligned} \tag{4}$$

where $b_{\mathrm{n}} = g_{\mathrm{n}}/g_1$ are the normalized coefficients of g_{n}. The terms of $|x(t)|^2 x(t)$ and $(x^*(t))^3$ represent the IMs and the counter CIMs, respectively. The nonlinearity of the mixer drives the LO harmonics to the sideband to become the CIMs. The 3rd, 7th,... order of CIMs are located at the lower sideband, where the 5th, 9th,... order of CIMs are located at the upper sideband.

Next is the analysis of the dependency between I/Q imbalance and mixer nonlinearities. Considering the I/Q imbalance, the BB signal $x(t)$ in (2) should be replaced by

$$x_{IQ}(t) = K_1 x(t) + K_2 x^*(t) \tag{5}$$

$$K_1 = \frac{(1 + g e^{-j\varphi})}{2}$$

$$K_2 = \frac{(1 - g e^{-j\varphi})}{2} \tag{6}$$

where g and φ are the gain and phase mismatches of the mixer, respectively, K_1 and K_2 are the mismatch coefficients [16]. Similarly, the MOD output $x_{\mathrm{MOD}}(t)$ is obtained as

$$\begin{aligned} x_{\mathrm{MOD}}(t) &= e^{j2\pi f_{LO}t}\left\{K_1 x(t) + 3K_1^2 K_2\left[\alpha|x(t)|^2 x(t) + \beta\left(x^*(t)\right)^3\right]\right\} \\ &\quad + e^{-j2\pi f_{LO}t} \\ &\quad \times \left\{K_2 x^*(t) + 3K_1 K_2^2\left[\alpha^*|x(t)|^2 x^*(t) + \beta^*\left(x(t)\right)^3\right]\right\} + \cdots \end{aligned} \tag{7}$$

where

$$\alpha = 3a_3\left(1 + 2|b_3|^2 + 2|b_5|^2 + 2b_3^* b_5\right)$$

$$\beta = a_3\left(b_3 + b_3^2 b_5^*\right)$$

The I/Q imbalance introduces the image of the signal, IMs and CIMs at the mirrored frequency with respect to f_{LO}. These tones

can further degrade the EVM of the transmitted signal. The nonlinearity of the MOD with nonlinear order L and finite memory length M can be modeled as

$$x_{\mathrm{MOD}}(n) = \sum_{l=1}^{2L-1} \frac{1}{2^l} \sum_{m_1=0}^{M} \sum_{m_2=0}^{M} \cdots \sum_{m_l=0}^{M} d_l(m_1, m_2, \ldots, m_l) \cdot \sum_{k=0}^{l} \binom{l}{k} \left(x(n-m_1)\right)^k \left(x^*(n-m_l)\right)^{l-k} \quad (8)$$

where $d_l(m_1, m_2, \ldots, m_l)$ is the lth-order kernel of the Volterra series, which indicates the dependency of the CIMs and I/Q imbalance. The nonlinear system can then be served as a multilinear FIR filter due to the linear combination property where the binomial expression $(x(n-m_1))^k (x^*(n-m_l))^{l-k}$ describes the IMs and CIMs.

B. RF Nonlinearities With Memory Effect

The nonlinearities of the TX are mainly generated by the PA which can also be modeled using a Volterra-series model. To simplify the analysis, the memory effect of the PA is ignored, and the Volterra-series of the PA is

$$y(t) = c_1 x_{\mathrm{MOD}}(t) + c_3 x_{MOD}^3(t) + \cdots \quad (9)$$

The even-order nonlinearity can be ignored since it cannot generate the tones at the in-band. For the 3rd-order nonlinearity, the terms $|x(t)|^2 x(t) e^{j2\pi f_{LO} t}$ and $|x(t)|^2 x^*(t) e^{-j2\pi f_{LO} t}$ are in-band while $[x(t)]^3 e^{j2\pi(3f_{LO})t}$ and $[x^*(t)]^3 e^{j2\pi(-3f_{LO}t)}$ are out-of-band and can be filtered. Thus, the simplified Volterra-series of the PA is given by

$$y(n) = \sum_{q=1}^{Q} \sum_{m_1=0}^{M} \sum_{m_2=0}^{M} \cdots \sum_{m_p=0}^{M} e_q(m_1, m_2, \ldots, m_p) \cdot \prod_{p_1=1}^{q} x_{\mathrm{MOD}}(n-m_{p_1}) \prod_{p_2=q+1}^{2q-1} x_{\mathrm{MOD}}^*(n-m_{p_2}) \quad (10)$$

where $x_{\mathrm{MOD}}(n)$ and $y(n)$ are the input and output of the PA, respectively. $e_q(m_1, m_2, \ldots, m_p)$ is the qth-order kernel of the Volterra series. m_{p_1} and m_{p_2} represent the memory effect of the PA. The term $\prod_{p_1=1}^{q} x_{\mathrm{MOD}}(n-m_{p_1}) \prod_{p_2=q+1}^{2q-1} x_{\mathrm{MOD}}^*(n-m_{p_2})$ represents the odd order nonlinearity. It should be noted that only the harmonics which can generate the term $|x_{\mathrm{MOD}}|^{2q} x_{\mathrm{MOD}}$ located around f_{LO} are considered in the PA model.

III. Proposed DPD for MOD + PA

In order to compensate the impairments of MOD + PA, CIM, I/Q imbalance and the PA nonlinearities are predistorted with the DDR method for relaxing the complexity of Volterra-series. Although the below analysis is based on the TV-band, the digital calibration can be extended to general wideband communications.

A. Parameter Extraction Methodology of the Proposed Predistorter

The nonlinearities of the CIM and the PA were discussed separately in Section II to identify the different effects. Each nonlinear block can be represented by one Volterra series in the BB model. Here, considering that two nonlinear Volterra-series are connected in tandem, the behavior can be modeled only by one Volterra-series [17]. As a result, comparing (8) and (10), the IM terms of the mixer overlap with the PA. In the overall predistorter, only IM terms of the PA have to be involved as the stronger nonlinearity effect by the PA, which are corresponded to the third and fourth terms [with parameter set (Q, M)] in (11). The remaining CIM and I/Q imbalance terms, which are corresponded to the first and second terms [with parameter set (L, M)] in (11), are stacked in parallel with the IM terms of the PA in the overall predistorter G as shown in Fig. 3. Note that the CIMs and I/Q imbalance terms are totally independent to the IM terms. For the proposed predistorter (Fig. 4), the number of coefficients has to be estimated first, as it increases exponentially if the description of the MOD and PA nonlinearities is based on the general Volterra-series. Here, the coefficients of the Volterra-series DPD are extracted by using the qth-order inverse predistorter with the DDR method to overcome the complexity of the general Volterra series [15], and can be represented as

$$\begin{aligned} u(n) &= \sum_{q=0}^{\frac{L-1}{2}} \sum_{i=0}^{M} g_{2q+1,1}(i) \sum_{k=0}^{2q+1} \binom{2q+1}{k} (y^*(n))^k (y(n-i))^{2q+1-k} \\ &\quad + \sum_{q=0}^{\frac{L-1}{2}} \sum_{i=0}^{M} g_{2q+1,2}(i) \sum_{k=0}^{2q+1} \binom{2q+1}{k} (y(n))^k \times (y^*(n-i))^{2q+1-k} \\ &\quad + \sum_{q=L+2}^{\frac{Q-1}{2}} \sum_{i=0}^{M} g_{2q+1,1}(i) \, |y(n)|^{2q} \, y(n-i) \\ &\quad + \sum_{q=L+2}^{\frac{Q-1}{2}} \sum_{i=0}^{M} g_{2q+1,2}(i) \, |y(n)|^{2(q-1)} \, y^2(n-i) y^*(n-i) \end{aligned} \quad (11)$$

where $u(n)$ is the post-inverse predistorted signal trained by $y(n)$, which is identical to the pre-inverse training [17]. r represents the order of dynamics involved in DPD. $g_{q,r}(\cdot)$ is the predistorted complex Volterra kernel of the system. In (11), the zeroth-order dynamic compensates the memoryless nonlinearity of the PA. The higher-order dynamics compensate the nonlinearity of the PA coupled with the nonlinear memory effect. For those that have $r > 3$ they can be eliminated in the model since the effects of dynamics are sufficiently small in a practical PA. Further, the predistorter is the DDR-based predistorter of [15], which can compensate the standalone PA nonlinearities, when considering $L = 0$. Based on the multi-linear properties of Volterra series, each $g_{q,r-1}(\cdot)$ of $u(n)$ is considered to be a coefficient, and is arranged to form a vector $\mathbf{g} = [g_{1,0}(0), \ldots, g_{q,0}(0), \ldots, g_{L,2}(M)]$. Thus, the vector $\mathbf{g}$ can directly be estimated by applying the Least Square (LS) solution, leading to

$$\hat{\mathbf{g}}_{\mathrm{LS}} = (\mathbf{Y}^{\boldsymbol{H}}\mathbf{Y})^{-1}\mathbf{Y}^{\boldsymbol{H}}\mathbf{x} \quad (12)$$

where $(\cdot)^H$ denotes the complex conjugate transpose. $\mathbf{x} = [x(0), \ldots, x(K-1)]$ with K-samples. The matrix $\mathbf{Y}$ includes all the product terms $y^{q-r}(n) \prod_{j=1}^{r} y(n-m_j)$ that correspond to all the rth-order of dynamic of the qth-order nonlinearity in each row according to the vector $\mathbf{g}$. Yet the accuracy of the LS solution becomes worse as the number of coefficients of the Volterra series increased in the model. The

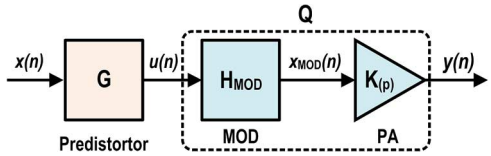

Fig. 3. Modeling the predistorter with the MOD + PA.

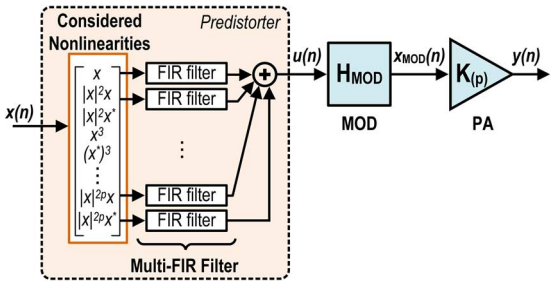

Fig. 4. Block schematic of the proposed DPD addressing both CIM, I/Q imbalance, and RF nonlinearities.

nonlinear system is then linearized after the qth-order inverse predistorter is connected in tandem [17]. Thus, the overall system S can be expressed as

$$S\left[x(n)\right] = x(n) + \sum_{m=q+1}^{\infty} S_m\left[x(n)\right] \tag{13}$$

where $S_{\mathrm{m}}[\cdot]$ is the nth-order Volterra operator of the system S. Note that $\sum_{q+1}^{\infty} S_m[\cdot]$ describes the $(q+1)$-order nonlinearity which is assumed to be negligible because S is fully linearized. Moreover, if the CIM terms are not involved, the coefficients of the IM terms in Volterra series will try to model those CIM terms by themselves. Then, the accuracy of the entire model would be obviously degraded.

B. Computational Complexity

The computational complexity of DPD arises mainly from the coefficients extraction stage with the LS matrix inversion and running complexity during online compensation. As the coefficients are usually extracted offline, the running complexity of the predistorter is an important consideration for implementation. Especially for the proposed predistorter, the performance limit is related to the increase of the running complexity after the CIMs and I/Q imbalance are included. In [18], the running complexity is analyzed with the number of floating point operations (FLOPs), which counts the number of operations in complex-value calculations, on the complexity-accuracy tradeoff. Note that only complex-value addition and multiplication of FLOPs are involved in the following analysis. For MOD + PA with the moderate memory effects of concern, a first-order dynamic $r = 1$ is chosen as the dynamic cross terms $(r > 1)$ is less effective. The proposed DPD in (11) related to three parameters, which include the order of nonlinearities of PA Q, the order of CIM L, and the memory length M, as discussed in Section II. The total complexity (C_{total}) of the proposed predistorter can be obtained from the sum of the constructing basis nonlinearities with FIR filters [18] which can be expressed as

$$C_{\mathrm{total}} = C_{\mathrm{basis}} + C_{\mathrm{filter}} \tag{14}$$

All the Volterra series based predistorters have a multi-FIR filter structure as discussed in Section II. The number of FIR filters is related to the considered nonlinearities. The complexity of the FIR filters (C_{filter}) with respect to the FLOPs can then be directly acquired by

$$C_{\mathrm{filter}}(Q, L, M) = 8 f_{\mathrm{proposed}}(Q, L, M) - 2 \tag{15}$$

where the total number of coefficients (f_{proposed}) in each kernel for proposed DPD is calculated as

$$f_{\mathrm{proposed}}(Q, L, M) = \frac{(L+3)(L+1)}{4} + (Q - L) + \frac{M(L+1)^2}{2} + 2M(Q - L) \tag{16}$$

In (16), the first two terms represent the memoryless DPD case as considering the CIMs provide $(L^2 - 1)/4$ and interaction of PA nonlinearities and I/Q imbalance provide $(Q + 1)$ terms. The last two terms correspond to $M \geq 1$, with CIMs provide $M(L+1) \cdot (L-3)/2$ and interaction of PA nonlinearities and I/Q imbalance provide $2M(Q+1)$ terms. The complexity of the constructing basis considering most nonlinearities can be calculated as

$$C_{\mathrm{basis}}(Q, M, L) = 9 + (M+1)(Q-1) + 6M\frac{(Q-3)}{2} + 3(M+1)(L-1) + \left[1 + 8\mathrm{M} + \frac{(L-3)}{2}\right]\frac{(L-3)}{2} \tag{17}$$

where $L \leq 5$ and L is odd. The complexity of initial constructions for $|x(n)|^2$ and $x^2(n)$ costs 9 FLOPs in (17). The basis construction for CIM and I/Q imbalance cost $3(M+1)(L-1) + [1 + 8M + (L-3)/2](L-3)/2$ while PA nonlinearities of DDR $(r = 1)$ cost $(M+1)(Q-1) + 6M(Q-3)/2$, as given in Table I, where each impairment versus basic construction, complexity, and number of coefficients are summarized. For the complexity of hardware, the focus should be the numbers of real-additions and multiplications on different impairments as listed in Table II. Comparing with [15] $(r = 2)$ that just can compensate the PA nonlinearities, the complexity of the proposed combinatorial DPD is more relaxed with DDR $(r = 2)$.

The complexity of the algorithm is traded with the accuracy of the compensation which can be analyzed by the ACLR and EVM. The ACLR can be minimized by choosing a larger Q, which is the PA nonlinear related order. Yet the improvement of the ACLR will be limited for $Q > 9$. Also, the EVM can be optimized by increasing the I/Q imbalance and CIMs related order L. If the order L is not sufficiently large, certain unwanted tones cannot be compensated which will be shown in Section IV-A. Generally, the EVM is satisfied when $L \leq 5$ for compensating

TABLE I
SUMMARY OF THE PROPOSED PREDISTORTER FOR IMPAIRMENTS AND ITS COMPLEXITY

Impairments	Basis Construction	Complexity of Basis	Number of Coefficients
CIM	$y^{l+1}(n)\,(y^*(n))^l$ $y^{l+2}(n)(y^*(n))^{l-1}\ldots$ $y^{2l}(n)$ with its conjugate	3(M+1)(L-1) + [1+8M+(L-3)/2] ·(L-3)/2	f(CIM)*
I/Q Imbalance	$\|y(n)\|^{2q}y^*(n-i)$	0	f(IQ)*
PA Nonlinearities	$\|y(n)\|^{2q}y(n-i)$	(M+1)(Q–1) +6M(Q–3)/2	f(PA)*

* : $\mathrm{f(CIM)} = (\mathrm{L}^2 - 1)/4 + (\mathrm{L}+1)(\mathrm{L}-3)\mathrm{M}/2$
$\mathrm{f(PA)} = \mathrm{f(IQ)} = (\mathrm{Q}+1)/2 + (\mathrm{Q}+1)(\mathrm{M})$

TABLE II
NUMBER OF REAL ADDITIONS AND MULTIPLICATIONS FOR EACH IMPAIRMENTS

Impairments	Number of real-additions	Number of real-multiplications
CIM	4f(CIM)-2+ (M+1)(L-1)	[1+8M+(L-3)/2](L-3)/2+4f(CIM) +2(M+1)(L-1)
I/Q Imbalance	4f(IQ)-2	4f(IQ)
PA Nonlinearities	4f(PA)-2+M(Q-3)	4f(PA)+2M(Q-3)

TABLE III
PERFORMANCE ESTIMATION OF THE PROPOSED DPD WITH M = 0 IN 65-NM CMOS AT 1.1 V AND 25 °C.

Predistorter	Power		No. of Gate	Area (mm^2)	No. of Clock cycle
	Leakage (mW)	Switching (mW)			
Proposed DPD	0.58	2.794	20295	0.1	14

the > -45 dBc CIMs of the mixers. Considering the FLOPs of the proposed DPD with $M = 0$ is 157, the power consumption, area and the number of gates are estimated through Cadence Encounter at 1.1 V and 25 °C in Table III. Thus, FLOPs of the proposed DPD with $M = 2$ is 639, the power consumption and area are roughly 4x higher with $M = 0$ case.

IV. SIMULATION AND MEASUREMENT RESULTS

The performance of the proposed DPD is evaluated by both simulations and measurements. By considering the OFDM signal as a multi-tone signal, a two-tone test is first exercised in simulations to show the effect of I/Q imbalance, CIM, and PA nonlinearities in the frequency domain. For measurements, both two-tone and OFDM-signal-based tests are included.

A. Simulation Results

The simulation setup based on all impairments of MOD + PA is evaluated in MATLAB as plotted in Fig. 5. 5% gain and 5° phase imbalances are assumed to represent the frequency-independent I/Q imbalance, which correspond to an initial image-rejection ratio (IRR) of roughly -30 dB. The g_n of LO in (1), which is considered as the Fourier series of a square wave, is mixed with the BB signal before harmonic rejection. Followed by the mixer nonlinearities, the overall nonlinearities in the mixing stage can be modeled as $a_1x + a_3x^3$ with $a_1 = 1$ and $a_3 = 0.002 - 0.0017j$. a_1 and a_3 are chosen such that the IM_3 of mixers is -45 dBc which matches with the practical values of the measured DUT. The FIR filter is added to model the frequency-dependent properties of the I/Q imbalance and the memory effect accompanying the PA. It is known as the filter bank in the two-block model (PA behavioral modeling [19]) and $h_{RF} = [1\ 0.7\ 0.035]$ is set. In the polynomial bank that provides the PA nonlinearities, a 5th-order polynomial with coefficients $c_1 = 14.974 + 0.052j$, $c_3 = -2.31 + 0.497j$ and $c_5 = -0.25 + 0.03j$ is modeled in (9) for a wideband nonlinear PA. LS solution is then applied to extract the coefficients of the predistorted data. Finally, the DPD is applied to the system.

With two tones at 1.2 and 1.5 MHz, the FFT under a grid of 6000-point are plotted in Fig. 6, where the sampling rate is 100 MHz. The memory effect is insignificant in the two-tone test, with $M = 0$ and the dynamic $r = 1$ is set. A predistorted

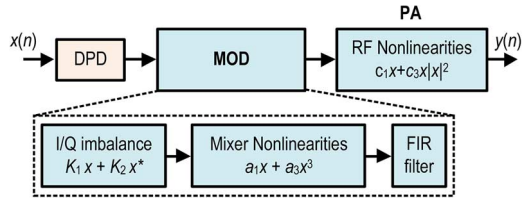

Fig. 5. Simulation setup for the MOD + PA.

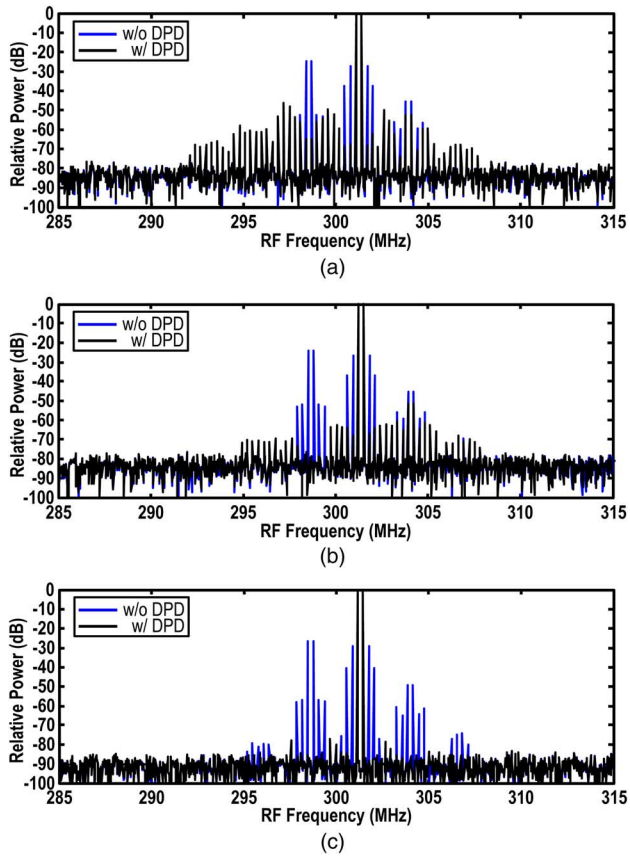

Fig. 6. Simulation results under two-tone tests for DPD including (a) RF nonlinearities; (b) I/Q imbalance and RF nonlinearities; (c) CIM, I/Q imbalance, and RF nonlinearities.

signal with standalone PA nonlinearities {$Q = 9$ and $L = 0$ in (11), similar to [15]} is applied to test the system as shown in Fig. 6(a). All the impairment terms created by I/Q imbalance and mixer nonlinearities are tried to be tracked by the PA nonlinearity terms $|x|^{2n}x$. The IM and I/Q imbalance terms are compensated up to -46 dBc. However, the unwanted tones are introduced due to the error extraction of the coefficients whenever $Q = 15$ in (11). In Fig. 6(b), with the PA nonlinearities and I/Q imbalance involved in the predistorter, the image tones are well-compensated when comparing with Fig. 6(a). The CIMs up to -53 dBc are not compensated. Comparatively, all the nonlinearities tones are reduced up to -73 dBc after the proposed DPD of (11) with $Q = 9$ and $L = 5$ is applied [Fig. 6(c)]. It is obvious that CIM, I/Q imbalance, and PA nonlinearities must be involved in the predistorter in order to compensate the impairments of MOD + PA accurately.

B. Measurement Results

The experimental setup is shown in Fig. 7. Here, the device under test (DUT) (Fig. 8) is a TV-band MOD + PA that was fabricated in 65-nm CMOS. The circuit design of the MOD

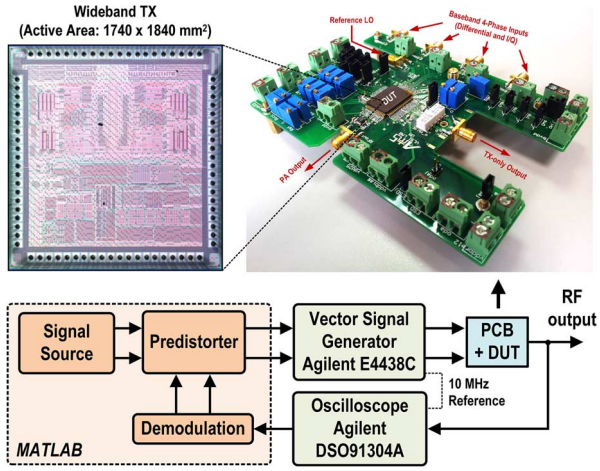

Fig. 7. Measurement setup. The DUT is a wideband TX designed and fabricated in a 65-nm CMOS technology.

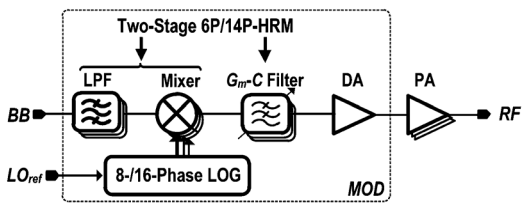

Fig. 8. Block diagram of the DUT.

is similar to [20], except the 2nd stage of the harmonic-rejection mixer, which is embedded in the $G_m - C$ filter to improve the matching and linearity in this prototype. Inside the DUT, the tested signals are passed through the BB passive-RC LPF, up-converted with a set of Gilbert mixer, and further filtered by a tunable $G_m - C$ filter. The RF signal is eventually boosted by a driver amplifier (DA) and an on-chip multi-transconductance linearized push-pull PA before driving the 50-Ω load. In this system, all the non-ideality of MOD will be generated as mentioned in Section II, such that it is a practical platform for testing the proposed DPD. It operates from 54 to 864 MHz with a +12-dBm OFDM average output power. The initial IRR measures −25 dB. The tested BB I/Q signals are generated by the Agilent E4438C. The output feedback signal from DUT is captured by an oscilloscope (Agilent DSO-91304A), which has roughly 8.5-bit amplitude resolution. The demodulation is conducted in MATLAB. In the parameter estimation, the resolution is limited by the output feedback signal of the oscillator. For concerning the fixed point effect, the 16-bit multiplication is chosen and truncated back to 8 bits after the multiplication in the matrix $\mathbf{Y}$. At 300 MHz RF, the result of a two-tone test at 1.2 and 1.5 MHz, is shown in Fig. 9. All expected impairments are measured in the DUT. The 5th, 7th, and even 9th order CIM terms are observed in the system. Extra coefficients are hence entailed to compensate these CIM terms in the two-tone case with $L = 7$and $Q = 11$. All the nonlinearities are suppressed up to −43 dBc after the proposed DPD is applied. Inversion error is introduced by the existence of the unexpected even harmonic terms [7], which come from the output matching network of the PA. Thus, the accuracy of the coefficients extraction is limited by that. The next test is to apply a 6-MHz bandwidth, 64-QAM, 2048-point OFDM digital-TV signal with a 96-MHz sampling rate. With a PAPR of 17 dB and thus a 9-dB power back-off, the

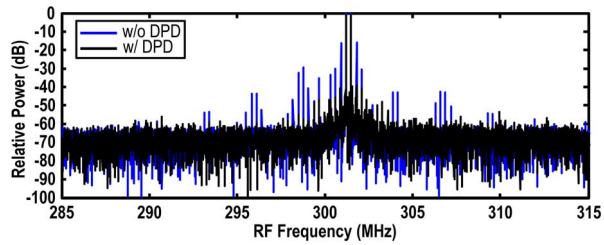

Fig. 9. Measurement result under two-tone tests.

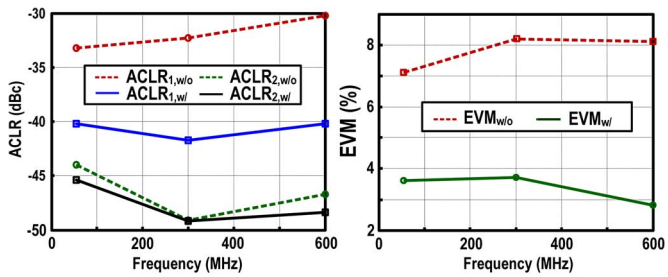

Fig. 10. Measurements with and without DPD: (a) ACLR at 1st and 2nd adjacent channels ($ACLR_1$ and $ACLR_2$), and (b) EVM. The input is a 64-QAM OFDM signal with 2048 points and a 6-MHz bandwidth.

measured output power is >10 dBm at 54, 300, and 600-MHz RF. Considering the moderate memory effect in the DUT, dynamic $r = 1$ is set. The optimum memory length $M = 2$ is found by sweeping M from 1 to 4. Unlike the two-tone signal, the higher-order CIM and frequency-dependent I/Q imbalance are overlapped as the symmetrical OFDM signal is applied. The CIM, I/Q imbalance, and RF nonlinearities are thus mixed together to affect the EVM and the 1st ACLR. For validating the performance of the proposed DPD, $L = 5$ and $Q = 9$ are set in (11) for optimal complexity-accuracy. The measured EVM (Fig. 10) at different RF is improved from 7.1% to 3.6% at 54 MHz, 8.2% to 3.7% at 300 MHz, and 8.1% to 2.8% at 600 MHz. For the ACLR, it is improved from −33.2 to −40.2 dBc, −32.3 to −41.7 dBc, and −30.2 to −40.2 dBc, respectively, for the same set of RF. The measured AM/AM and AM/PM, with and without the proposed DPD, are plotted in Fig. 11. As expected, nonlinearity, memory effects and CIM have been well-compensated in both AM/AM and AM/PM.

To further study the CIM, the predistorter for compensating I/Q imbalance and PA nonlinearities in (11) are measured with $Q = 15$ and $M = 5$. The improvement of EVM is degraded to 4.8% at 54-MHz, 5.2% 300-MHz, and 5.6% 600-MHz RF. The reduction of ACLR is insignificant as the CIM terms act more like the memory effect of PA. For the AM/AM and AM/PM curves (Fig. 12), the convergence of the AM/AM is dominated by the interaction of CIM and memory effect of PA. The incomplete compensation on nonlinearities, especially at 54-MHz RF, is thus observed in the AM/AM curve.

A one-shot wideband calibration is measured by applying the proposed predistorter at 300-MHz RF. The EVM is improved to 4.1% at 54-MHz and to 4.2% at 600-MHz RF. The ACLR stays around −39.8 to −39.9 dBc, as most nonlinearities are cancelled in the spectrum. From the measured AM/AM and AM/PM curves (Fig. 13), the degradation in AM/AM, AM/PM, and EVM performance are mainly originated from the frequency-dependent memory effect. Still, the performance can fulfill the IEEE 802.11af standard, offering a new alternative to

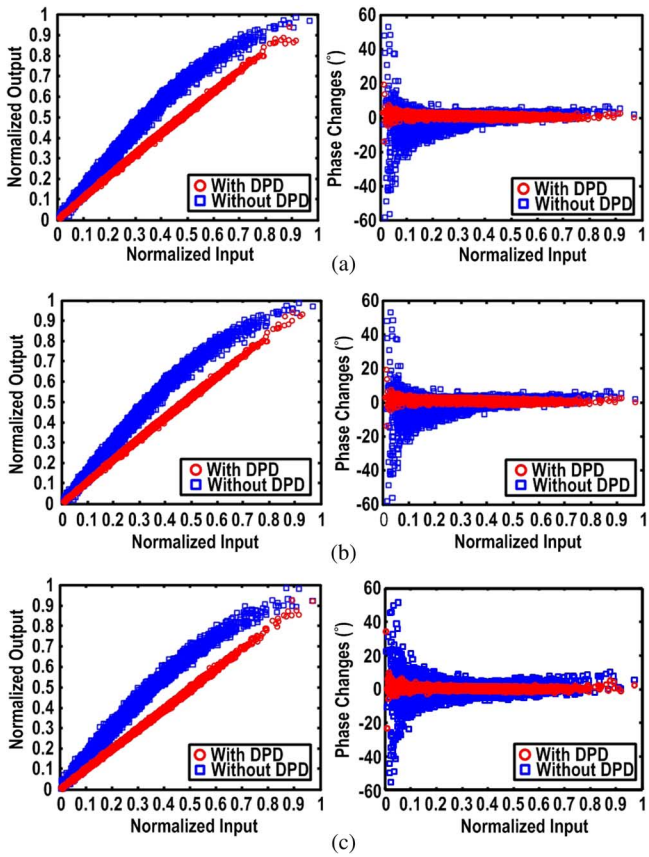

Fig. 11. Measured AM/AM and AM/PM curves of the proposed DPD at (a) 54 MHz; (b) 300 MHz; and (c) 600 MHz RF.

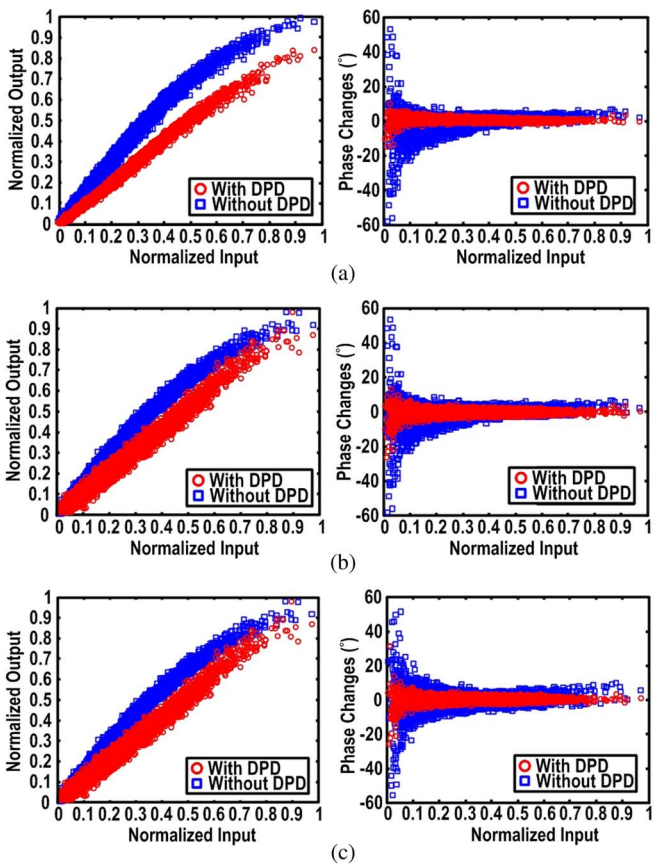

Fig. 12. Measured AM/AM and AM/PM curves of the proposed DPD with L = 0 at (a) 54 MHz; (b) 300 MHz; and (c) 600 MHz RF.

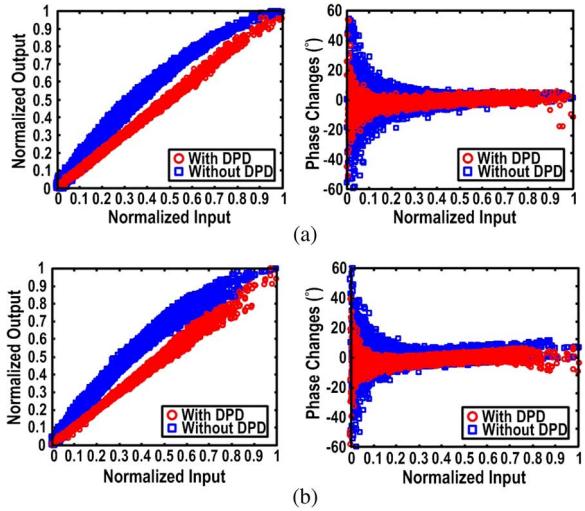

Fig. 13. Measured AM/AM and AM/PM curves of the proposed DPD at (a) 54 MHz and (b) 600 MHz RF, using the wideband characteristic measured at 300 MHz.

reduce the number of compensation and computational power while keeping a satisfactory performance.

V. Conclusions

A combinatorial impairment-compensation DPD for a sub-GHz IEEE 802.11af WLAN wideband TX has been proposed. It addresses the frequency-dependent I/Q imbalance, CIM and RF nonlinearities of the MOD + PA. By analyzing the system model via Volterra series, the predistorter can effectively compensate those impairments by stacking the model of MOD in parallel with that for the PA nonlinearities. The running complexity in terms of FLOP is analyzed, which is more relaxed when compared with the existing predistorter (it addresses only the PA nonlinearities). Both simulation and measurement results validate the performance of the pre-distorter under individual and one-shot wideband calibrations.

References

[1] IEEE 802.11af WLAN MAC & PHY Specifications, Dec. 2013.
[2] J. Kim, S. Lee, and S. Kim *et al.*, "A 54–862-MHz CMOS transceiver for TV-band white-space device applications," *IEEE Trans. Microw. Theory Tech.*, vol. 59, no. 4, pp. 966–977, Apr. 2011.
[3] S. Subhan, E. A. M. Klumperink, and B. Nauta, "Towards suppression of all harmonics in a polyphase multipath transmitter," in *Proc. IEEE Int. Symp. Circuits Syst. (ISCAS)*, 2011, pp. 2185–2188.
[4] J. Vuolevi, *Distortions in RF Power Amplifier*. Norwood, MA, USA: Artech House, 2003.
[5] L. Ding, Z. Ma, D. R. Morgan, M. Zierdt, and G. T. Zhou, "Compensation of frequency-dependent gain/phase imbalance in predistortion linearization systems," *IEEE Trans. Circuits Syst. I, Reg. Papers*, vol. 55, no. 1, pp. 390–397, Feb. 2008.
[6] H. Cao, A. S. Tehrani, C. Fager, T. Erikkson, and H. Zirath, "I/Q imbalance compensation using a nonlinear modeling approach," *IEEE Trans. Microw. Theory Tech.*, vol. 57, no. 3, pp. 513–518, Mar. 2009.
[7] M. Collados, H. Zhang, B. Tenbroek, and H.-H. Chang, "A low-current digitally predistorted direct-conversion transmitter with 25% duty-cycle passive mixer," *IEEE Trans. Microw. Theory Tech.*, vol. 62, no. 4, pp. 726–731, Apr. 2014.
[8] A. Mirzaei, D. Murphy, and H. Darabi, "Analysis of direct-conversion IQ transmitters with 25% duty-cycle passive mixers," *IEEE Trans. Circuits Syst. I, Reg. Papers*, vol. 58, no. 10, pp. 2318–2331, Oct. 2011.
[9] D. Mirri *et al.*, "A modified Volterra series approach for nonlinear dynamic systems modeling," *IEEE Trans. Circuits Syst. I, Fundam. Theory Appl.*, vol. 49, no. 8, pp. 1118–1128, Aug. 2002.

[10] X. Huang and M. Caron, "Efficient transmitter self-calibration and amplifier linearization techniques," in *Proc. IEEE Int. Circuits Syst. Symp. (ISCAS)*, 2007, pp. 265–268.

[11] S. W. Chung, J. W. Holloway, and J. L. Dawson, "Energy-efficient digital predistortion with lookup table training using analog Cartesian feedback," *IEEE Trans. Microw. Theory Tech.*, vol. 56, no. 10, pp. 2248–2258, Oct. 2008.

[12] L. Anttila, P. Handel, and M. Valkama, "Joint mitigation of power amplifier and I/Q modulator impairments in broadband direct-conversion transmitters," *IEEE Trans. Microw. Theory Tech.*, vol. 58, no. 4, pp. 730–739, Apr. 2010.

[13] C. Eun and E. J. Powers, "A new volterra predistorter based on the indirect learning architecture," *IEEE Trans. Signal Process.*, vol. 45, no. 1, pp. 223–227, Jan. 1997.

[14] D. R. Morgan, Z. Ma, L. Kim, M. G. Zierdt, and J. Pastalan, "A generalized memory polynomial model for digital predistortion of RF power amplifiers," *IEEE Trans. Signal Process.*, vol. 54, no. 10, pp. 3852–3860, Oct. 2006.

[15] A. Zhu, P. J. Draxler, J. J. Yan, T. J. Brazil, D. F. Kimball, and P. M. Asbeck, "Open-loop digital predistorter for RF power amplifiers using dynamic deviation reduction-based Volterra series," *IEEE Trans. Microw. Theory Tech.*, vol. 56, no. 7, pp. 1524–1534, Jul. 2008.

[16] L. Anttila, M. Valkama, and M. Renfors, "Circularity-based I/Q imbalance compensation in wideband direct-conversion receivers," *IEEE Trans. Microw. Theory Tech.*, vol. 57, no. 4, pp. 2009–2113, Jul. 2008.

[17] M. Schetzen, *The Volterra and Wiener Theories of Nonlinear System*. New York: Wiley, 1980.

[18] A. S. Tehrani, H. Cao, S. Afsardoost, T. Eriksson, M. Isaksson, and C. Fager, "A comparative analysis of the complexity/accuracy tradeoff in power amplifier behavioral models," *IEEE Trans. Microw. Theory Tech.*, vol. 58, no. 6, pp. 1510–1520, Jun. 2010.

[19] D. Schreurs, M. O'Droma, A. A. Goacher, and M. Gadringer, *RF Power Amplifier Behavioral Modeling*. Cambridge, U.K.: Cambridge Univ. Press, 2009.

[20] K.-F. Un, P.-I. Mak, and R. P. Martins, "A 53-to-75-mW, 59.3-dB HRR, TV-band white-space transmitter using a low-frequency reference LO in 65-nm CMOS," *IEEE J. Solid-State Circuits*, vol. 48, no. 9, pp. 2078–2089, Sep. 2013.

Chak-Fong Cheang (S'13) received his B.Sc. and his M.Sc. degree in the Department of Engineering Science, National Cheng Kung University (NCKU), Tainan, Taiwan, in 2008, 2010. He is currently working toward the Ph.D. degree at the UM State-Key Laboratory of Analog and Mixed-Signal VLSI and Faculty of Science and Technology (ECE) from University of Macau, Macao, China.

His research interests are digital predistortion and digital mitigation on RF impairment and field-programmable gate-array (FPGA)-based embedded signal processing.

Ka-Fai Un (S'09) received his B.Sc. degree in electrical engineering from National Taiwan University (NTU), in 2007, and his M.Sc. degree in electrical and electronics engineering from the University of Macau (UM), Macao, China, in 2009. He received his Ph.D. degree at the UM State-Key Laboratory of Analog and Mixed-Signal VLSI and Faculty of Science and Technology (ECE) in 2014, where he is currently a Postdoctoral Researcher.

His research interests are switched-capacitor circuits and wireless circuits design. In 2003, Dr. Un won the Macau Mathematics Olympics and represented Macau in the Chinese Mathematics Olympics (CMO) and the International Mathematics Olympics (IMO), in Changsha and Tokyo, respectively. He is the recipient of the 2008 APCCAS Merit Student Paper Certificate.

Wei-Han Yu (S'09) received the B.Sc., and M.Sc. degrees in Electrical and Electronics Engineering from the University of Macau, Macao SAR, China, in 2010 and 2012, respectively, where he is currently working toward the Ph.D. degree at the UM State-Key Laboratory of Analog and Mixed- Signal VLSI and Faculty of Science and Technology (ECE) from University of Macau, Macao, China.

His research focus on RF and mm-wave transmitter, power amplifier, digital predistortion, and EM modeling for next-generation mobile communications.

Pui-In Mak (S'00–M'08–SM'11) received the Ph.D. degree from University of Macau (UM), Macao SAR, China, in 2006. He is currently Associate Professor at UM, and Associate Director (Research) of the *State-Key Laboratory of Analog and Mixed-Signal VLSI*. His research interests are on analog and RF circuits and systems for wireless, biomedical and physical chemistry applications.

His involvements with IEEE are: Distinguished Lecturer ('14–'15) and Member of Board-of-Governors ('09–'11) of IEEE Circuits and Systems Society (CASS); Editorial Board Member of IEEE Press ('14–'16); Senior Editor of IEEE JOURNAL ON EMERGING AND SELECTED TOPICS IN CIRCUITS AND SYSTEMS ('14–'15); Associate Editor of IEEE TRANSACTIONS ON CIRCUITS AND SYSTEMS—PART I (TCAS-I) ('10–'11, 14'-); Associate Editor of IEEE TRANSACTIONS ON CIRCUITS AND SYSTEMS—PART II (TCAS-II) ('10–'13), and Guest Editor of IEEE RFIC VIRTUAL JOURNAL ('14).

Prof. Mak received IEEE DAC/ISSCC Student Paper Award '05; IEEE CASS Outstanding Young Author Award '10; National Scientific and Technological Progress Award '11; Best Associate Editor for TCAS-II '12–'13. In 2005, he was decorated with the *Honorary Title of Value* for scientific merits by the Macau Government.

Rui P. Martins (M'88–SM'99–F'08) was born in April 30, 1957. He received the B.S. (5-years), the M.S., and the Ph.D. degrees, as well as the Habilitation for Full-Professor in electrical engineering and computers from the Department of Electrical and Computer Engineering, Instituto Superior Técnico (IST), TU of Lisbon, Portugal, in 1980, 1985, 1992, and 2001, respectively. He has been with the Department of Electrical and Computer Engineering (DECE)/IST, TU of Lisbon, since October 1980.

Since 1992, he is also with the Department of Electrical and Computer Engineering, Faculty of Science and Technology (FST), University of Macau (UM), Macao, China, where he has been a Chair-Professor since August 2013. At FST he was the Dean of the Faculty from 1994 to 1997 and he has been Vice-Rector of the University of Macau since 1997, being Vice-Rector (Research) since 2008. He created in 2003 the *Analog and Mixed-Signal VLSI Research Laboratory* of University of Macau, elevated in January 2011 to State Key Laboratory of China (the 1st in Engineering in Macao), being its Founding Director.

Prof. Martins was the Founding Chairman of IEEE Macau Section (2003–2005), and IEEE Macau Joint-Chapter on CAS/COM (2005–2008) [2009 World Chapter of the Year of the IEEE CAS Society]. He was Vice-President for Region 10 of IEEE CASS (2009–2011), Vice-President (World) Regional Activities and Membership of IEEE CASS (2012–2013), and Associate Editor of IEEE TRANSACTIONS ON CIRCUITS AND SYSTEMS—PART II (TCAS-II) (2010–2013), nominated Best Associate Editor for 2012 to 2013. Plus, he was a member of the IEEE CASS Fellow Evaluation Committee (Classes of 2013 and 2014). He was the recipient of 2 government decorations: the Medal of Professional Merit from Macao Government (Portuguese Administration) in 1999, and the Honorary Title of Value from Macao SAR Government (Chinese Administration) in 2001. In July 2010 was elected, unanimously, as Corresponding Member of the Portuguese Academy of Sciences (in Lisbon), being the only Portuguese Academician living in Asia.